PDGFRB mutation and tyrosine kinase inhibitor resistance in Ph-like acute lymphoblastic leukemia

Supplementary methods and figures for Yingchi Zhang et al.

Supplementary Methods

Sequencing and mutation analysis

Whole genome sequencing was performed on the bone marrow samples from 3-time points during the treatment course, i.e., at diagnosis, the chemotherapy refractory, and relapse after imatinib treatment, as well as the sample from saliva as control. Paired-end sequencing was performed on an Illumina Hiseq X ten with 150bp read length. Reads were aligned to UCSC hg19.GRch37 using Burrows-Wheeler Aligner[1], filtered for duplicate reads, and analyzed for quality using Genome Analysis Toolkit[2]. Mutect[3], Varscan2[4] and CASpoint (an in-house software) were used to call somatic variants, followed by ANNOVAR[5] to perform variant functional annotation. The nonsynonymous mutations with VAF>0.3 in at least one sample and detected by at least two kinds of variant-calling software are defined as high confidence mutations, and used to generate the mutational profile. Somatic structural variants and copy number variants were detected by CREST[6] and CONSERTING[7], respectively. RNA sequencing was performed on RNA extracted from the same bone marrow samples at 3-time points as WGS using the Illumina Hiseq2500 in high output mode with a 2×101-bp pair-end reads. Reads were aligned using TopHat2[8]. Gene fusions were generated using TopHat-Fusion[9], SOAPfuse[10], and deFuse[11]. The raw sequencing data reported in this paper have been deposited in the Genome Sequence Archive[12] in BIG Data Center[13], Beijing Institute of Genomics (BIG), Chinese Academy of Sciences, under accession numbers CRA000588 that are publicly accessible at http://bigd.big.ac.cn/gsa.

In vitro cytokine-independent growth assay in Ba/F3 cells and *Arf*$^{-/-}$ bone marrow cells

The full-length *AGGF1-PDGFRB* and *EBF1-PDGFRB* coding sequence were amplified from primary ALL patient samples and cloned into the GV365-IRES-GFP lentiviral vector. *AGGF1-* or *EBF1-PDGFRB*^{C843G} was site-directed mutated using Agilent mutagenesis kit and lentiviral supernatants were produced by transient

transfection of HEK-293T cells using calcium phosphate. Ba/F3 cells were maintained in medium supplemented with 10 ng/ml recombinant mouse interleukin 3 (IL3) (PeproTech). Ba/F3 cells were transduced with lentiviral supernatants expressing the above fusion genes. GFP positive cells were sorted 48 hours after transduction and maintained in IL3 medium for another 24 hours, and then washed three times and grown in the absence of cytokine. *Arf*$^{-/-}$ bone marrow cells were harvested from two 6-10 weeks old female *Arf*$^{-/-}$ mice (C57/BL6) and transduced with the above lentivirus in BCM5 media without any supplemental cytokines. Cell growth and viability were monitored daily by Trypan blue using a TC10 automated cell counter (BIO-RAD). Each experiment was performed three times.

Tyrosine kinase inhibitor cytotoxicity

Ba/F3 cells or *Arf*$^{-/-}$ cells over-expressing *AGGF1-PDGFRB* or *EBF1-PDGFRB* or their *PDGFRB*^{C843G} mutant forms were incubated with increasing concentrations of TKI for 72 hours (*AGGF1-PDGFRB* [imatinib, dasatinib, ponatinib, and nilotinib] and *EBF1-PDGFRB* [imatinib and nilotinib]: 10 μM, 2.5 μM, 0.625 μM, 0.15625 μM, 0.039063 μM, 0.009766 μM, and 0.002441 μM; *EBF1-PDGFRB* [dasatinib and ponatinib]: 1 μM, 0.25 μM, 0.0625 μM, 0.015625 μM, 0.0039063 μM, 0.0009766 μM, and 0.0002441 μM;), after which cell viability was measured using MTT assay. Experiments were performed in triplicate and repeated at least three times and results were plotted using Graph Prism 5.

Droplet digital PCR

The QX200 Droplet Digital PCR System (Bio-Rad) was used to simultaneously detect frequency of mutation of *PDGFRB*^{C843G}, *IKZF1*^{G158S}, *IKZF1* Del2-7 and *IKZF1* Del4-7 in a duplex reaction. The ddPCR workflow was described as previous[14]. Roughly 20 ng of gDNA was digested was assayed in a Taqman ddPCR reaction for in a final volume of 20 μL containing: 2×ddPCR Mastermix (Bio-Rad), 20×primer and probes (final concentrations of 900 and 250 nM, respectively). The primers and probes used for *PDGFRB* and *IKZF1* gene were as followed: 5'-GGAGATGTAATTCGAGTCC-3' (*PDGFRB* forward); 5'-GGTCTTTCCCCACAATTG-3' (*PDGFRB* reverse); 5'-6-FAM-

AGGCCAAAGTCACAGATCTTGACCAG-BHQ1-3' (*PDGFRB*-wt); 5'-VIC-AGGCCAAAGTCACCGATCTTGACCAG-BHQ1-3' (*PDGFRB*-mut); 5'-CTTCCAGTGCAATCAGTG -3' (*IKZF1* forward); 5'- CAGAGGTGGCATTTGAAG -3' (*IKZF1* reverse); 5'-6-FAM- CACCCAGAAGGGCAACCTGC -BHQ1-3' (*IKZF1*-wt); 5'-VIC- CACCCAGAAGAGCAACCTGC -BHQ1-3' (*IKZF1*-mut); 5'-CTTACAAGAAGAGAAACA-3' (*IKZF1* Del2-7 forward); 5'-ACCCTAATTAGGATGTATCTT-3' (*IKZF1* Del2-7 reverse); 5'-AGAAGTCTGGAGTCTGTC-3' (*IKZF1* Del4-7 forward); 5'-CCATTTTGTCTAGAGAGTC-3' (*IKZF1* Del4-7 reverse). We partitioned each reaction mixture into approximately 20,000 droplets with a droplet generator (Bio-Rad) and then cycled with the following conditions: 95℃×10 min (1 cycle), 94℃×30 s and 60℃×1 min (40 cycles), 98℃×10 min (1 cycle), and 4 ℃ hold. This condition was chosen after performing an annealing temperature gradient to ensure the two genes amplification. Data analysis of the ddPCR reads was carried out using QuantaSoft analysis software (Bio-Rad). Absolute quantification of the *PDGFRB* and *IKZF1* gene for each sample was then calculated in every patient. Experiments were performed in triplicate and repeated at least three times and results were plotted using Graph Prism5.

Western blotting and immunofluorescence staining

Ba/F3 cells with empty vector, *AGGF1-PDGFRB*, *EBF1-PDGFRB*, *BCR-ABL* and *AGGF1-PDGFRB*^{mut} were washed twice with ice-cold PBS and then lysed using lysis buffer. Total cell lysate (20 μg) was heated at 95 °C for 5 min in sample buffer, subjected to PAGE, and then electrotransferred onto nitrocellulose membranes. Detection was performed using HRP-conjugated secondary antibodies and enhanced chemiluminescence. Akt (#9272), Phospho-Akt (Ser473) (#4060), p44/42 MAPK(Erk1/2) (#9102), Phospho-p44/42 MAPK (Erk1/2) (Thr202/Tyr204) (#9288), Stat5 (#94205), Phospho-Stat5 (Tyr694) (#9314) and H3 (#4499) antibodies were purchased from Cell Signaling Technology. For the immunofluorescence procedure, *AGGF1-PDGFRB* and *EBF1-PDGFRB* Ba/F3 cells were fixed with 4%

paraformaldehyde solution, permeabilized with 0.25% Triton X-100, washed twice with PBS and blocked with 1% BSA for 30 min at room temperature. The samples were then incubated with FoxO1 antibody diluted 1:100 in 1% BSA for 2 h at room temperature. Primary antibodies were detected using secondary antibody (donkey anti-rabbit Alexa Fluor plus 555, Cat # A32727, Invitrogen) diluted 1:200 with1% BSA for 1 h at room temperature. The samples were then washed twice. After 5ug/ml DAPI was added, the samples were examined under an Axio Imager Z2 fluorescence microscope (ZEISS).

Structural modeling

Structural model of *PDGFRB* kinase domain was generated using Phyre 2.0[15] with KIT kinase bound to ponatimid (PDB ID 4UOI). Sequence identity between template and target protein was 60%, and confidence level of generated model was assessed as 100%. To verify orientation of respective inhibitors, final model was superposed with structures for cSrc kinase with dasatinib (3G5D), and with JAK2 bound to NVP-BSK805 (3UGC). Interactions of *PDGFRB* proteins (wild type and C843G mutant) with small molecules were assessed using Arpeggio[16].

Statistical analysis

Student's t test was used for comparisons between two groups, and ANOVA was used for multiple groups. All results represent the average of at least three independent experiments and are expressed as the mean ± SD. $P<0.05$ was considered significant.

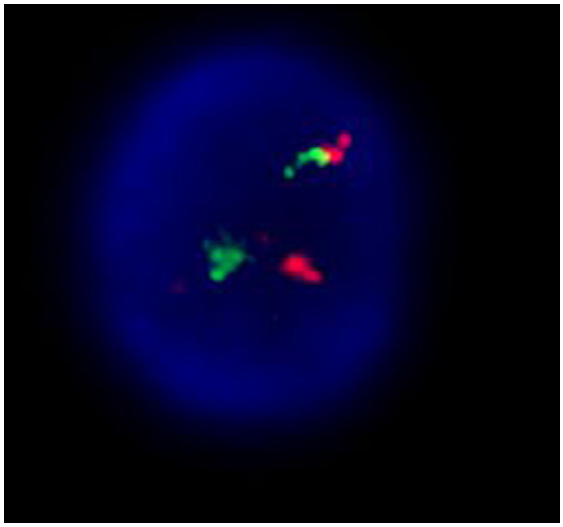

Supplementary Figure 1. *PDGFRB* rearrangement in diagnostic ALL blasts. Fluorescence in situ hybridization (FISH) was performed using a commercial *PDGFRB* break-apart probe to detect the rearrangement of *PDGFRB*.

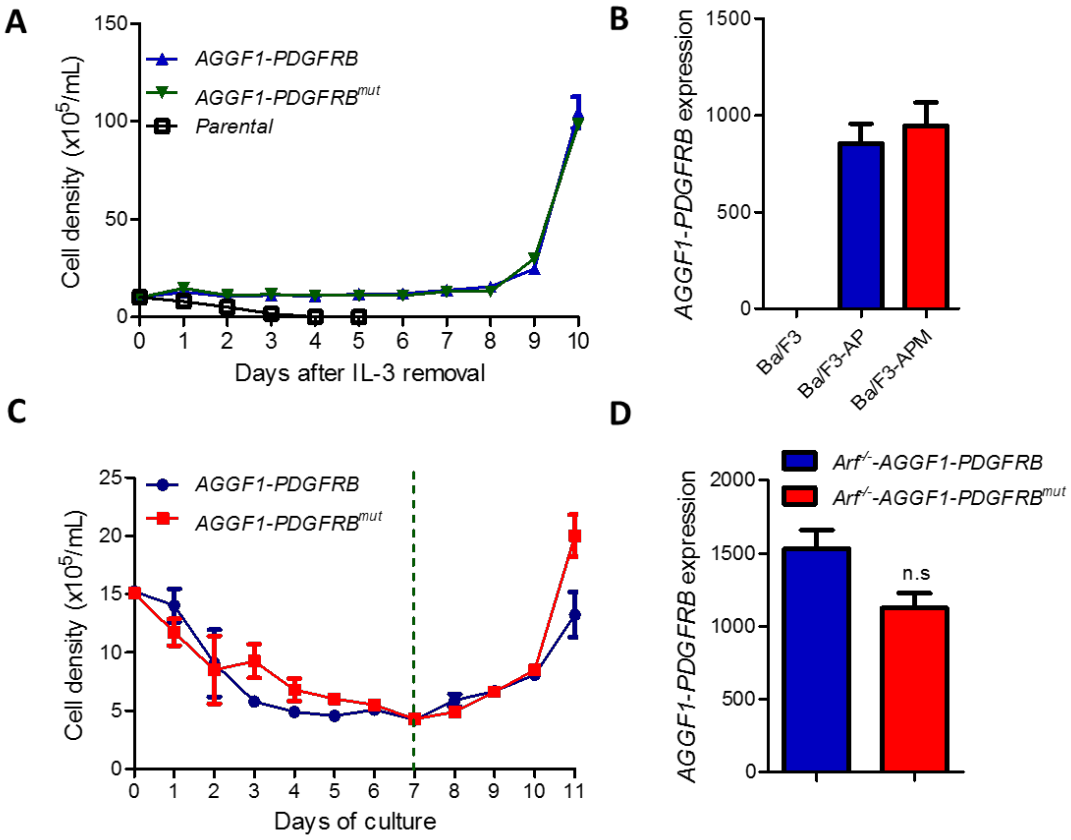

Supplementary Figure 2. *AGGF1-PDGFRB* fusion with the *C843G* mutation (*AGGF1-PDGFRB*^{mut}) also conferred cytokine-independent growth of Ba/F3 and *Arf*$^{-/-}$ bone marrow cells.

(A) *AGGF1-PDGFRB* with mutation *PDGFRB*^{C843G} promoted proliferation of Ba/F3 cells independent of IL-3, in a fashion similar to wildtype fusion gene. (B) Expression of *AGGF1-PDGFRB* and *AGGF1-PDGFRB*^{mut} in Ba/F3 cells. (C) Proliferation of *Arf*$^{-/-}$ bone marrow cells with *AGGF1-PDGFRB* or *AGGF1-PDGFRB*^{mut}. (D) Expression of *AGGF1-PDGFRB* and *AGGF1-PDGFRB*^{mut} in *Arf*$^{-/-}$ cells. All experiments were performed in triplicate.

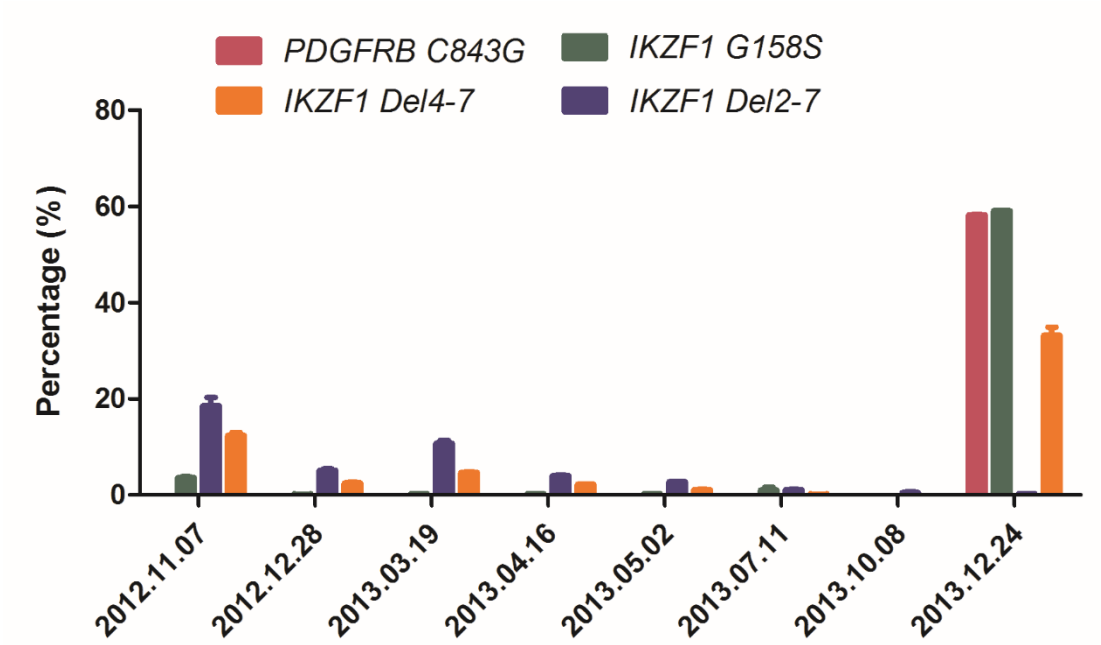

Supplementary Figure 3. Quantification of *PDGFRB*^{C843G}, *IKZF1*^{G158S}, *IKZF1 Del2-7 and IKZF1 Del4-7* in 8 longitudinal samples between ALL diagnosis and relapse, using droplet digital PCR.

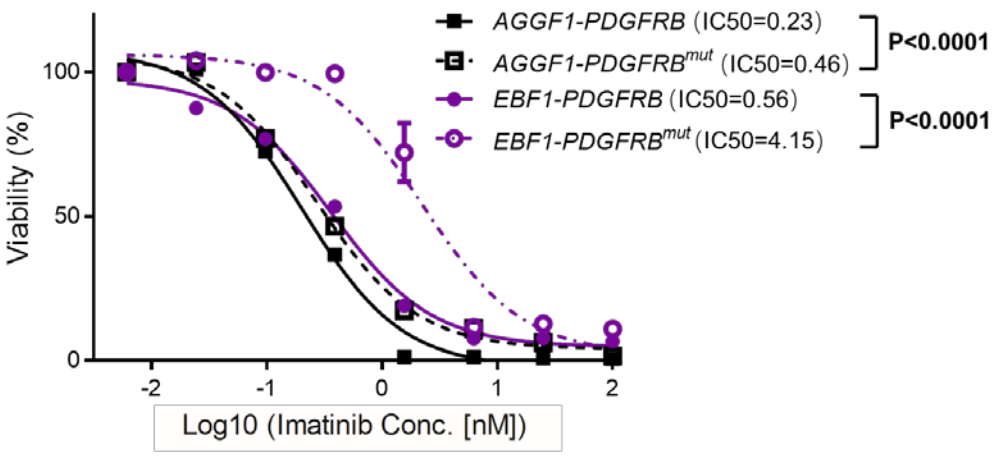

Supplementary Figure 4. *PDGFRB*^{C843G} mutation and imatinib resistance in Ba/F3 cells. Imatinib drug sensitivity of Ba/F3 cells with *AGGF1-PDGFRB*, *EBF1-PD*GFRB, *AGGF1-PDGFRB*^{mut}, or *EBF1-PDGFRB*^{mut} was evaluated by MTT assay. All experiments were performed in triplicate.

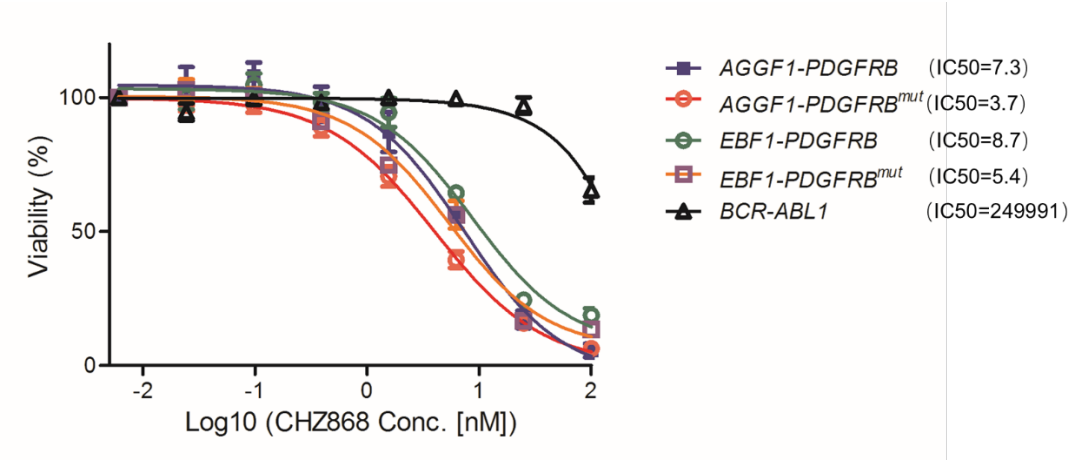

Supplementary Figure 5. *PDGFRB* fusion (either with *AGGF1* or *EBF1*) but not *BCR-ABL1* was associated with sensitivity to CHZ868. CHZ868 sensitivity of Ba/F3 cells with *AGGF1-PDGFRB*, *EBF1-PD*GFRB, *AGGF1-PDGFRB*^{mut}, *EBF1-PDGFRB*^{mut} or *BCR-ABL1* was evaluated by MTT assay. All experiments were performed in triplicate.

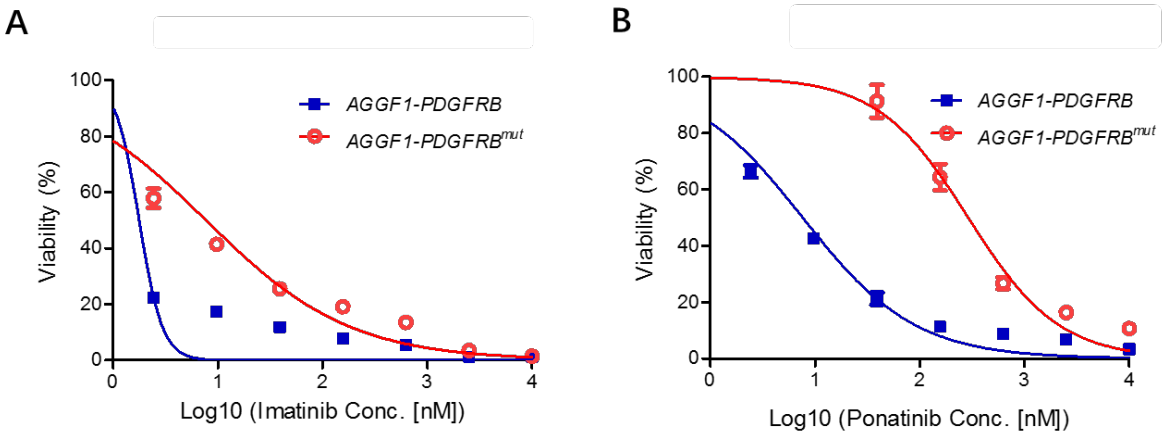

Supplementary Figure 6. *PDGFRB*^{C843G} mutation and TKI resistance in *Arf*$^{-/-}$ leukemia cells. MTT assay of *Arf*$^{-/-}$ cells with *AGGF1-PDGFRB* or *AGGF1-PDGFRB*^{mut} upon treatment of dasatinib (A) and ponatinib (B). All experiments were performed in triplicate.

References

1. Li H, Durbin R. Fast and accurate long-read alignment with Burrows–Wheeler transform. *Bioinformatics*. 2010;26(5):589-595.
2. DePristo MA, Banks E, Poplin RE, et al. A framework for variation discovery and genotyping using next-generation DNA sequencing data. *Nature genetics*. 2011;43(5):491-498.
3. Cibulskis K, Lawrence MS, Carter SL, et al. Sensitive detection of somatic point mutations in impure and heterogeneous cancer samples. *Nat Biotechnol*. 2013;31(3):213-219.
4. Koboldt DC, Zhang Q, Larson DE, et al. VarScan 2: Somatic mutation and copy number alteration discovery in cancer by exome sequencing. *Genome Research*. 2012;22(3):568-576.
5. Wang K, Li M, Hakonarson H. ANNOVAR: functional annotation of genetic variants from high-throughput sequencing data. *Nucleic Acids Research*. 2010;38(16):e164-e164.
6. Wang J, Mullighan CG, Easton J, et al. CREST maps somatic structural variation in cancer genomes with base-pair resolution. *Nature methods*. 2011;8(8):652-654.
7. Chen X, Gupta P, Wang J, et al. CONSERTING: integrating copy-number analysis with structural-variation detection. *Nat Methods*. 2015;12(6):527-530.
8. Kim D, Pertea G, Trapnell C, Pimentel H, Kelley R, Salzberg SL. TopHat2: accurate alignment of transcriptomes in the presence of insertions, deletions and gene fusions. *Genome Biology*. 2013;14(4):R36.
9. Kim D, Salzberg SL. TopHat-Fusion: an algorithm for discovery of novel fusion transcripts. *Genome Biology*. 2011;12(8):R72.
10. Jia W, Qiu K, He M, et al. SOAPfuse: an algorithm for identifying fusion transcripts from paired-end RNA-Seq data. *Genome Biology*. 2013;14(2):R12.
11. McPherson A, Hormozdiari F, Zayed A, et al. deFuse: An Algorithm for Gene Fusion Discovery in Tumor RNA-Seq Data. *PLoS Computational Biology*. 2011;7(5):e1001138.
12. Wang Y, Song F, Zhu J, et al. GSA: Genome Sequence Archive. *Genomics, Proteomics & Bioinformatics*. 2017;15(1):14-18.
13. Big Data Center Members. The BIG Data Center: from deposition to integration to translation. *Nucleic Acids Research*. 2017;45(Database issue):D18-D24.
14. Hindson BJ, Ness KD, Masquelier DA, et al. High-Throughput Droplet Digital PCR System for Absolute Quantitation of DNA Copy Number. *Analytical Chemistry*. 2011;83(22):8604-8610.
15. Kelley LA, Mezulis S, Yates CM, Wass MN, Sternberg MJE. The Phyre2 web portal for protein modelling, prediction and analysis. *Nature protocols*. 2015;10(6):845-858.
16. Jubb HC, Higueruelo AP, Ochoa-Montaño B, Pitt WR, Ascher DB, Blundell TL. Arpeggio: A Web Server for Calculating and Visualising Interatomic Interactions in Protein Structures. *Journal of Molecular Biology*. 2017;429(3):365-371.